will be used where n^* represents the nominal (constant) thrust-to-weight ratio required if the descent was vertical. Again, in previous studies this profile would be tracked by adding a simple linear feedback law with a high gain to guarantee tracking. The required thrust-to-weight ratio $\tilde{n}$ is then written as

$$\tilde{n} = n^* + \lambda(v - \tilde{v}) \tag{8}$$

This control will provide adequate tracking, however, only if the gain λ is large enough to compensate for the nonlinear terms in the vehicle dynamics represented by Eqs. (1). Using nonlinear transformation methods it will now be demonstrated that the desired descent profile can be tracked in a systematic manner using slant range, slant range rate, and local vertical information.

A pseudocontrol will again be defined as

$$u \triangleq v - \tilde{v} \tag{9}$$

where $\tilde{v}$ is the required vehicle velocity defined as a function of the measured slant range. Taking the first derivative of the pseudocontrol, the thrust-to-weight ratio appears as before, viz.,

$$\dot{u} = \dot{v} - \tilde{v}'(R)\dot{R} \tag{10}$$

where, again, the slant range and range rate can be measured with a body-fixed Doppler radar strapped to the $-z$ body axis of the descent vehicle. The required thrust-to-weight ratio $\tilde{n}$ can then be obtained as

$$\tilde{n} = \cos\psi + (1/g)\{-\tilde{v}'(R)\dot{R} + \kappa(v - \tilde{v})\} \tag{11}$$

To implement this control requires measurements of slant range and range rate, vehicle velocity, and the descent angle ψ. This corresponds to a knowledge of the local vertical. Such information can be derived from a horizon sensor or even from inertial navigation system estimates updated from the vehicle predescent attitude.[3] Importantly, the control ensures that the error dynamics behave exactly as a damped first-order system, allowing tracking of the desired decent profile from a large domain of the system state space.

A typical descent profile is shown in Fig. 2a for a starting condition well away from the desired descent contour. The contour is defined by Eq. (7) with a nominal thrust-to-weight ratio n^* of 2.35. The initial vehicle velocity is some 50% larger than the required velocity on the descent contour. It can be seen from Fig. 2b that the initial error is damped by throttling the descent engine so that the desired descent contour is accurately tracked. A 5-g axial load limiter has been included. Since the vehicle velocity is monotonically decreasing, however, the desired descent contour is eventually reached and subsequently tracked.

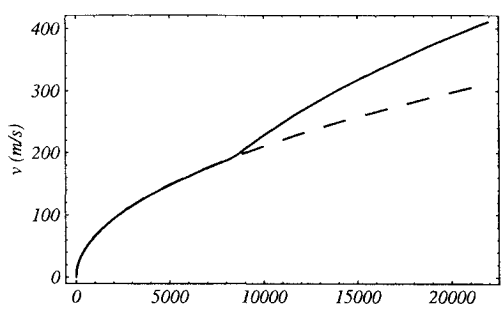

Fig. 2a Velocity-slant range profile tracking: — —, desired profile, and ——, actual profile.

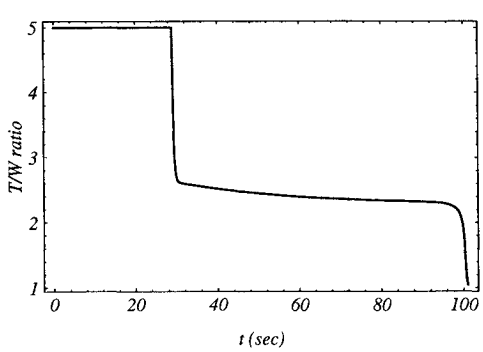

Fig. 2b Commanded thrust-to-weight ratio T/W.

Conclusions

It has been demonstrated that previous studies of descent contour tracking have much in common with contemporary nonlinear transformation methods. Rather than enforcing a high-gain, linear control over the desired decent contour, feedback linearization methods allow descent contour tracking in a systematic manner. The error dynamics of the systems are designed to exactly follow a damped first-order linear system, ensuring tracking from off the desired descent contour. Using this method a descent guidance law has been derived that requires only simple sensor measurements to implement. This scheme may allow simple guidance with less complex sensors for low-cost soft landing of payloads on the lunar surface.

References

[1]Cheng, R. K., "Lunar Terminal Guidance," *Lunar Missions and Exploration*, Wiley, New York, 1964, pp. 308–355.

[2]Citron, S. J., Dunn, S. E., and Meissinger, H. F., "A Terminal Guidance Technique for Lunar Landing," *AIAA Journal*, Vol. 2, No. 3, 1964, pp. 503–509.

[3]Cheng, R. K., "Terminal Guidance for a Mars Softlander," *Proceedings of the 8th International Symposium on Space Technology and Science* (Tokyo, Japan), 1969, pp. 855–865.

[4]Cheng, R. K., "Design Consideration for Surveyor Guidance," *Journal of Spacecraft and Rockets*, Vol. 3, No. 11, 1966, pp. 1569–1576.

[5]Ingoldby, R. N., "Guidance and Control System Design of the Viking Planetary Lander," *Journal of Guidance, Control, and Dynamics*, Vol. 1, No. 3, 1978, pp. 189–196.

[6]Mease, K. D., and Kremer, J. P., "Shuttle Entry Guidance Revisited Using Nonlinear Geometric Methods," *Journal of Guidance, Control, and Dynamics*, Vol. 17, No. 6, 1994, pp. 1350–1356.

[7]Kassing, D., "LEDA (Lunar European Assessment Study) Final Report," European Space Research and Technology Center, LEDA-RP-95-02, Noordwijk, The Netherlands, June 1995.

Analytical Solution for Dynamic Analysis of a Flexible L-Shaped Structure

Hyochoong Bang*
Korea Aerospace Research Institute, Daejon 305-600, Republic of Korea

I. Introduction

DYNAMIC analysis of flexible structures usually starts from mathematical modeling of the structures. Both analytical approaches[1] and finite dimensional approximations[2] are used to derive the mathematical model. For simple structures, the analytical approach is an attractive choice in terms of the solution accuracy. In the rather general cases, however, the approximation techniques are frequently used due to computational advantage.

Analytical solutions rely upon solving boundary value problems represented by characteristic equations.[1,2] In spite of the difficulty of solving characteristic equations, the analytical approaches yield well-behaved shape functions as solutions for low-order variables, such as displacements and slopes, as well as higher order variables, such as strain and stress. On the other hand, approximation

Received April 12, 1995; revision received June 20, 1995; accepted for publication June 25, 1995.

*Research Scientist, Koreasat Group. Member AIAA.

methods suffer from less numerical difficulties.[2] The approximation methods, at the cost of computational advantage, raise a question on the accuracy of the solution. In particular, significant errors are unavoidable when higher order variables, such as strain and stress, are evaluated by the approximation methods.

In this Note, analytical solutions for an L-shaped beam are developed. The L-shaped beam, which consists of two elastic domains, has been used as a space structure model in some previous studies,[3,4] such as flexible space antenna and reflector. The L-shaped structure is usually subject to a large deflection maneuver compared to a single elastic domain structure. In particular, the second structure motion is dynamically coupled to the tip motion of the base structure, which results in large deflection on the base structure. Note that the scope is still restricted to small elastic displacement of the base structure.

II. Derivation of Analytical Solution

Equations of Motion

The linearized equations of motion for the L-shaped beam as shown in Fig. 1 are given in the following form[1]:

$$\rho_1 \ddot{y}_1 + E_1 I_1 \frac{\partial^4 y_1}{\partial x_1^4} = 0 \tag{1a}$$

$$\rho_2(\ddot{y}_2 + x_2\ddot{\alpha}) + E_2 I_2 \frac{\partial^4 y_2}{\partial x_2^4} = 0 \tag{1b}$$

and the boundary conditions are

$$\begin{aligned} y_1(x_1, t) &= \frac{\partial y_1}{\partial x_1} = 0, \qquad \text{at} \quad x_1 = 0 \\ y_2(x_2, t) &= \frac{\partial y_2}{\partial x_2} = 0, \qquad \text{at} \quad x_2 = 0 \end{aligned} \tag{2a}$$

$$\begin{aligned} \int_0^{l_2} \rho_2 \, dx_2 \ddot{y}_1(l_1) &= E_1 I_1 \frac{\partial^3 y_1}{\partial x_1^3}\bigg|_{l_1} \\ \int_0^{l_2} \rho_2 |(x_2\ddot{\alpha} + \ddot{y}_2) x_2 \, dx_2 &= -E_1 I_1 \frac{\partial^2 y_1}{\partial x_1^2}\bigg|_{l_1} \end{aligned} \tag{2b}$$

$$E_2 I_2 \frac{\partial^2 y_2}{\partial x_2^2}\bigg|_{l_2} = 0, \qquad E_2 I_2 \frac{\partial^3 y_2}{\partial x_2^3}\bigg|_{l_2} = 0 \tag{2c}$$

where the subscripts 1 and 2 represent parameters of the base and second structures, respectively. In addition, ρ is the linear mass density, y elastic deflection, EI beam rigidity, and α is the slope at the tip of the base structure

$$\alpha = \frac{\partial y_1(x_1, t)}{\partial x_1}\bigg|_{x_1 = l_1}$$

Derivation of Characteristic Equation

To derive a characteristic equation, we introduce finite dimensional discretization[2,4]

$$y_1(x_1, t) = X_1(x_1)T_1(t), \qquad y_2(x_2, t) = X_2(x_2)T_2(t)$$

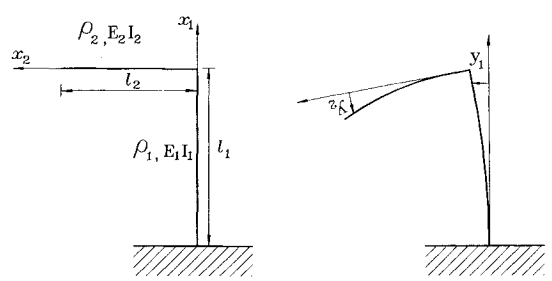

Fig. 1 Schematic configuration of the L-shaped beam.

From Eq. (1a)

$$\rho_1 X_1(x_1)\ddot{T}_1(t) + E_1 I_1 \frac{d^4 X_1(x_1)}{dx_1^4} T_1(t) = 0 \tag{3}$$

That is,

$$\frac{\ddot{T}_1(t)}{T_1(t)} = -\frac{E_1 I_1}{\rho_1} \frac{X_1''''(x_1)}{X_1(x_1)} = -\omega^2 \tag{4}$$

where $()''''$ denotes the fourth derivative of $()$ with respect to x_1 and ω is introduced to represent a harmonic motion of the time-dependent function $T(t)$; in this case, ω is the natural frequency of the system. The solution for Eq. (4) is well known as

$$\begin{aligned} X_1(x_1) &= C_1 \sin\gamma_1 x_1 + C_2 \cos\gamma_1 x_1 + C_3 \sinh\gamma_1 x_1 \\ &\quad + C_4 \cosh\gamma_1 x_1 \end{aligned} \tag{5}$$

where

$$\gamma_1^4 = \omega^2 \rho_1 / E_1 I_1$$

On the other hand, using Eq. (1b) and the definition of $y_2(x_2, t)$, it follows that:

$$\rho_2[X_2(x_1)\ddot{T}_2(t) + x_2 X'(l_1)\ddot{T}_1(t)] + E_2 I_2 X_2''''(x_2) T_2(t) = 0 \tag{6}$$

In addition, from the boundary conditions,

$$\int_{l_{0_2}}^{l_2} \rho_2[x_2 X_1'(l_1)\ddot{T}_1(t) + X_2(x_2)\ddot{T}_2(t)] x_2 \, dx_2 = -E_1 I_1 X_1''(l_1) T_1(t)$$

For the preceding equation to be valid for any time t, the functions $T_1(t)$ and $T_2(t)$ should satisfy $T_1(t) = T_2(t)$ as well as

$$\ddot{T}_1(t) = -\omega^2 T_1(t), \qquad \ddot{T}_2(t) = -\omega^2 T_2(t)$$

Therefore, Eq. (6) can be rewritten as

$$\rho_2\left[-X_2(x_2)\omega^2 - x_2 X_1'(l_1)\omega^2\right] + E_2 I_2 X_2''''(x_2) = 0 \tag{7}$$

The solution to Eq. (7) becomes

$$\begin{aligned} X_2(x_2) &= D_1 \sin\gamma_2 x_2 + D_2 \cos\gamma_2 x_2 + D_3 \sinh\gamma_2 x_2 \\ &\quad + D_4 \cosh\gamma_2 x_2 - X_1'(l_1) x_2 \end{aligned} \tag{8}$$

where γ_2 is defined as

$$\gamma_2^4 = \omega^2 \rho_2 / E_2 I_2$$

Applying the geometric boundary conditions for $X_1(x_1)$ in Eq. (2a), we obtain

$$X_1(0) = C_2 + C_4 = 0 \qquad X_1'(0) = \gamma_1(C_1 + C_3) = 0$$

Consequently, $X_1(x_1)$ is simplified into

$$X_1(x_1) = C_1(\sin\gamma_1 x_1 - \sinh\gamma_1 x_1) + C_2(\cos\gamma_1 x_1 - \cosh\gamma_1 x_1) \tag{9}$$

Also, application of the geometric boundary conditions on $X_2(x_2)$ yields

$$X_2(0) = D_2 + D_4 = 0 \tag{10a}$$

$$\begin{aligned} X_2'(0) &= \gamma_2(D_1 + D_3) - \gamma_1(\cos\gamma_1 l_1 - \cosh\gamma_1 l_1) C_1 \\ &\quad + \gamma_1(\sin\gamma_1 l_1 + \sinh\gamma_1 l_1) C_2 = 0 \end{aligned} \tag{10b}$$

Hence, $X(x_2)$ can be rewritten as

$$\begin{aligned} X_2(x_2) &= D_1 \sin\gamma_2 x_2 + D_2(\cos\gamma_2 x_2 - \cosh\gamma_2 x_2) \\ &\quad + D_3 \sinh\gamma_2 x_2 - X_1'(l_1) x_2 \end{aligned} \tag{11}$$

Next, the natural boundary conditions in Eqs. (2b) and (2c) lead us to the following expressions:

$$E_1 I_1 X_1'''(l_1) = -m_2\omega^2 X_1(l_1)$$

$$-E_1 I_1 X_1''(l_1) = \int_0^{l_2} \rho_2\left[-x_2 X_1'(l_1)\omega^2 - \omega^2 X_2(x_2)\right]x_2\,dx_2 \quad (12a)$$

$$E_2 I_2 X_2''(l_2) = 0, \qquad E_2 I_2 X_2'''(l_2) = 0 \quad (12b)$$

where $m_2 = \int_0^{l_2} \rho_2\,dx_2$ is the total mass of the second structure. Once the two shape functions in Eqs. (9) and (11) are substituted into Eqs. (12), a set of algebraic equations are derived in a matrix form as follows:

$$\begin{bmatrix} A_{11} & A_{12} & 0 & 0 & 0 \\ 0 & 0 & A_{23} & A_{24} & A_{25} \\ 0 & 0 & A_{33} & A_{34} & A_{35} \\ A_{41} & A_{42} & A_{43} & 0 & A_{45} \\ A_{51} & A_{52} & A_{53} & A_{54} & A_{55} \end{bmatrix} \begin{Bmatrix} C_1 \\ C_2 \\ D_1 \\ D_2 \\ D_3 \end{Bmatrix} = \begin{Bmatrix} 0 \\ 0 \\ 0 \\ 0 \\ 0 \end{Bmatrix} \quad (13)$$

where one of the geometric boundary conditions in Eq. (10) is also included in the matrix equation. In addition, each parameter inside the matrix is defined as

$$A_{11} = \gamma_1^3(-\cos\gamma_1 l_1 - \cosh\gamma_1 l_1) + (m_2/E_1 I_1)\omega^2(\sin\gamma_1 l_1 - \sinh\gamma_1 l_1)$$

$$A_{12} = \gamma_1^3(\sin\gamma_1 l_1 - \sinh\gamma_1 l_1) + (m_2/E_1 I_1)\omega^2(\cos\gamma_1 l_1 - \cosh\gamma_1 l_1)$$

$$A_{23} = -\sin\gamma_2 l_2, \qquad A_{24} = -\cos\gamma_2 l_2 - \cosh\gamma_2 l_2$$

$$A_{25} = \sinh\gamma_2 l_2, \qquad A_{31} = -\cos\gamma_2 l_2$$

$$A_{32} = \sin\gamma_2 l_2 - \sinh\gamma_2 l_2, \qquad A_{33} = \cosh\gamma_2 l_2$$

$$A_{41} = -\gamma_1(\cos\gamma_1 l_1 - \cosh\gamma_1 l_1)$$

$$A_{42} = -\gamma_1(-\sin\gamma_1 l_1 - \sinh\gamma_1 l_1)$$

$$A_{43} = \gamma_2, \qquad A_{45} = \gamma_2$$

$$A_{51} = E_1 I_1 \gamma_1^2(\sin\gamma_1 l_1 + \sinh\gamma_1 l_1)$$

$$A_{52} = E_1 I_1 \gamma_1^2(\cos\gamma_1 l_1 + \cosh\gamma_1 l_1)$$

$$A_{53} = -\rho_2\omega^2\left[\left(1/\gamma_2^2\right)\sin\gamma_2 l_2 - (l_2/\gamma_2)\cos\gamma_2 l_2\right]$$

$$A_{54} = -\rho_2\omega^2\left[\left(1/\gamma_2^2\right)\cos\gamma_2 l_2 + (l_2/\gamma_2)\sin\gamma_2 l_2 - (l_2/\gamma_2)\sinh\gamma_2 l_2 + \left(1/\gamma_2^2\right)\cosh\gamma_2 l_2\right]$$

$$A_{55} = -\rho_2\omega^2\left[(l_2/\gamma_2)\cosh\gamma_2 l_2 - \left(1/\gamma_2^2\right)\sinh\gamma_2 l_2\right]$$

For a nontrivial solution to exist, the determinant of the coefficient matrix of Eq. (13) should be equal to zero. After some algebra and simplification, the resulting characteristic equation is in the form

$$\gamma_2(1 + \cos\gamma_2 l_2 \cosh\gamma_2 l_2)\left[\gamma_1^3(1 + \cos\gamma_1 l_1 \cosh\gamma_1 l_1) - \left(m_2\omega^2/E_1 I_1\right)(\sin\gamma_1 l_1 \cosh\gamma_1 l_1 - \sinh\gamma_1 l_1 \cos\gamma_1 l_1)\right] = 0 \quad (14)$$

Equation (14) can be solved for ω, i.e., the natural frequency of the system. It is worthwhile to note that this characteristic equation reflects dynamic couplings between the two elastic domains. Especially, the γ_2, a single factor in the equations, can be explained by the tip motion of the base structure. The dynamic coupling term $m_2\omega^2/E_1 I_1$ in the equation becomes dominant as the mass m_2 of the second structure increases, which is physically a feasible phenomenon. Also, we can find, in Eq. (14)

$$1 + \cos\gamma_2 l_2 \cosh\gamma_2 l_2 = 0$$

is a well-known equation for a simple beam with one end fixed and the other end free.[5] Therefore, the new characteristic equation provides useful physical insight. Since the equation is a nonlinear transcendental equation, a numerical technique is necessary to find the solution. As is commonly known, some difficulty is expected finding solutions for higher modes.

Table 1 Configuration parameters

Symbol	Value
l_1, m	4.249
l_2, m	2.215
ρ_1, kg/m	0.0045
ρ_2, kg/m	0.0060
$E_1 I_1$, N-m^2	0.0267
$E_2 I_2$, N-m^2	0.0147

Table 2 Numerical results

Mode no.	Frequency, Hz	ω^2, rad^2/s^2	Error
1	0.36	5.026×10^0	-9.933×10^{-19}
2	2.28	2.045×10^2	-2.294×10^{-12}
3	3.14	3.901×10^2	-3.520×10^{-11}
4	3.87	5.918×10^2	-6.988×10^{-9}
5	5.89	1.371×10^3	6.202×10^{-7}
6	6.16	1.498×10^3	5.237×10^{-7}
7	8.33	2.745×10^3	-5.665×10^{-4}

III. Example Problem

An application of the result developed in the preceding section is made to a model system. The numerical data for the model system are provided in Table 1. First seven natural frequencies are computed numerically by solving the characteristic equation (14) using Newton–Raphson method. In this particular case, the seventh mode is the highest mode that can be obtained without significant numerical error, which can be evaluated by substituting the converged value into the original equation, Eq. (14). It turns out that the computer code size is much shorter compared to using a finite element method. Table 2 presents the computed natural frequencies and numerical error for each mode.

IV. Conclusion

Analytical solution for the eigenvalue problem of a flexible L-shaped beam is obtained. The double elastic domains structure produced a characteristic equation, where the nonlinear coupling effects between each domain are well represented. This analytical result can be used as a benchmark test for numerical solutions of the similar structures. Also, the approach taken in this study can be extended into other multiple domain flexible structures.

References

[1]Thomson, R. C., "A Perturbation Approach to Control of Rotational and Translational Maneuvers of Flexible Space Vehicles," M.S. Dissertation, Dept. of Engineering Mechanics, Virginia Polytechnic Inst. and State Univ., Blacksburg, VA, April 1985.

[2]Kim, Y., Junkins, J. L., and Kurdila, A. J., "On the Consequence of Certain Modeling Approximations in Dynamics and Control of Flexible Space Structures," *Proceedings of the 33rd Structural Dynamics and Materials Conference* (Dallas, TX), AIAA, Washington, DC, 1992, pp. 1173–1184.

[3]Agrawal, B. N., and Bang, H., "Active Vibration Control of Flexible Space Structures by using Piezoelectric Sensors and Actuators," *Proceedings of the 14th Biennial ASME Conference* (Albuquerque, NM), American Society of Mechanical Engineers, New York, 1993, pp. 169–179.

[4]Bang, H., and Agrawal, B. N., "A Generalized Second Order Compensator for Vibration Control of Flexible Structures," *Proceedings of the AIAA/ASME/ASCE/AHS/ASC 35th Structures, Structural Dynamics, and Materials Conference* (Hilton Head, SC), AIAA, Washington, DC, 1994, pp. 2438–2448 (AIAA Paper 94-1626).

[5]Meirovitch, L., *Elements of Vibration Analysis*, McGraw–Hill, New York, 1986, pp. 161–166.